Research Article | Vol. 6, No. 10 | 1 Oct 2016 | OPTICAL MATERIALS EXPRESS 3045

Optical Materials EXPRESS

0.6–1.6 THz band spectroscopy of organic thermally activated delayed fluorescence materials

HARUNOBU TAKEDA,[1] CONG CHEN,[1] TAKESHI KOMINO,[2,3] HIROAKI YOSHIOKA,[1] YUJI OKI,[1,3,*] AND CHIHAYA ADACHI[2,3]

[1]*Graduate School and Faculty of Information Science and Electrical Engineering, Kyushu University, 744 Motooka, Nishi-ku, Fukuoka 819-0395, Japan*
[2]*Center for Organic Photonics and Electronics Research (OPERA), Kyushu University, 744 Motooka, Nishi-ku, Fukuoka 819-0395, Japan*
[3]*Japan Science and Technology Agency (JST), ERATO, Adachi Molecular Exciton Engineearing Project, Kyushu University, 744 Motooka, Nishi-ku, Fukuoka 819-0395, Japan*
[*]*oki@ed.kyushu-u.ac.jp*

Abstract: Newly developed thermally activated delayed fluorescence (TADF) materials are attractive for application in efficient displays. Five TADF materials, including PXZ-TRZ and four carbazolyl dicyanobenzene (CDCB) derivatives of 4CzTPN, 4CzTPN – Ph, 2CzPN, and 4CzIPN, were investigated using terahertz spectroscopy in the 0.60 – 1.60 THz range. While PXZ-TRZ was almost transparent, the carbazolyl dicyanobenzene (CDCB) derivatives, especially 4CzIPN, exhibited intrinsic absorption features. Comparing these results with density functional theorem calculations, each absorption feature was clarified to originate from the intramolecular motions of the carbazole units.

© 2016 Optical Society of America

OCIS codes: (040.2235) Far infrared or terahertz; (160.2540) Fluorescent and luminescent materials; (160.4760) Optical properties.

References and links

1. M. Mizukami, S. Oku, S. I. Cho, M. Tatetsu, M. Abiko, M. Mamada, T. Sakanoue, Y. Suzuri, J. Kido, and S. Tokito, "A Solution-Processed Organic Thin-Film Transistor Backplane for Flexible Multiphoton Emission Organic Light-Emitting Diode Displays," IEEE Electron Device Lett. **36**(8), 1 (2015).
2. J. T. Smith, S. Member, B. O. Brien, Y. K. Lee, E. J. Bawolek, S. Member, and J. B. Christen, "Application of Flexible OLED Display Technology for Electro-Optical Stimulation and / or Silencing of Neural Activity," J. Disp. Technol. **10**(6), 514–520 (2014).
3. H. Uoyama, K. Goushi, K. Shizu, H. Nomura, and C. Adachi, "Highly efficient organic light-emitting diodes from delayed fluorescence," Nature **492**(7428), 234–238 (2012).
4. H. Tanaka, K. Shizu, H. Miyazaki, and C. Adachi, "Efficient green thermally activated delayed fluorescence (TADF) from a phenoxazine-triphenyltriazine (PXZ-TRZ) derivative," Chem. Commun. **48**(93), 11392 (2012).
5. J. Li, T. Nakagawa, J. MacDonald, Q. Zhang, H. Nomura, H. Miyazaki and C. Adachi, "Highly Efficient Organic Light-Emitting Diode Based on a Hidden Thermally Activated Delayed Fluorescence Channel in a Heptazine Derivative," Adv. Matter. **25**, 3319–3323 (2013).
6. Q. Zhang, B. Li, S. Huang, H. Nomura, H. Tanaka and C. Adachi, "Efficient blue organic light-emitting diodes employing thermally activated delayed fluorescence," Nature Photonics **8**, 326–332 (2014).
7. C. Adachi, M. A. Baldo, M. E. Thompson and S. R. Forrest, "Nearly 100% internal phosphorescence efficiency in an organic light-emitting device," J. Appl. Phys. **90**, 5048–5051 (2001)
8. C. L. Linfoot, M. J. Leitl, P. Richardson, A. F. Rausch, O. Chepelin, F. J. White, H. Yersin, and N. Robertson, "Thermally Activated Delayed Fluorescence (TADF) and Enhancing Photoluminescence Quantum Yields of [CuI(diimine)(diphosphine)]+ Complexes–Photophysical, Structural, and Computational Studies," Inorg. Chem. **53**(20), 10854–10861 (2014).
9. C. Murawski, K. Leo, and M. C. Gather, "Efficiency roll-off in organic light-emitting diodes," Adv. Mater. **25**(47), 6801–6827 (2013).
10. P. Schouwink, A. Schäfer, C. Seidel, and H. Fuchs, "The influence of molecular aggregation on the device properties of organic light emitting diodes," Thin Solid Films **372**(1-2), 163–168 (2000).
11. S. Wang, Y. Zhang, W. Chen, J. Wei, Y. Liu, and Y. Wang, "Achieving high power efficiency and low roll-off OLEDs based on energy transfer from thermally activated delayed excitons to fluorescent dopants," Chem. Commun. **51**, 11972–11975 (2015).

#270599 http://dx.doi.org/10.1364/OME.6.003045
Journal © 2016 Received 15 Jul 2016; revised 26 Aug 2016; accepted 26 Aug 2016; published 2 Sep 2016

Optical Materials EXPRESS

12. G. Zhao, B. Yu, and C. Zhang, "Terahertz spectroscopic investigation of four kinds of vitamins," Appl. Phys. **106**(10), 1–6 (2009).
13. T. M. Korter, R. Balu, M. B. Campbell, M. C. Beard, S. K. Gregurick and E. J. Heiweil, "Terahertz spectroscopy of solid serine and cysteine," Chem. Phys. Lett. **418**(1–3), 65–70 (2006)
14. C. J. Strachan, T. Rades, D. A. Newnham, K. C. Gordon, M. Pepper, and P. F. Taday, "Using terahertz pulsed spectroscopy to study crystallinity of pharmaceutical materials," Chem. Phys. Lett. **390**(1-3), 20–24 (2004).
15. P. D. Cunningham, N. N. Valdes, F. A. Vallejo, L. M. Hayden, B. Polishak, X. H. Zhou, J. Luo, A. K. Y. Jen, J. C. Williams, and R. J. Twieg, "Broadband terahertz characterization of the refractive index and absorption of some important polymeric and organic electro-optic materials," J. Appl. Phys. **109**(4), 1–5 (2011).
16. M. Leahy-Hoppa, M. Fitch, X. Zheng, L. Hayden, and R. Osiander, "Wideband terahertz spectroscopy of explosives," Chem. Phys. Lett. **434**(4-6), 227–230 (2007).
17. Y. Cai, I. Brener, J. Lopata, J. Wynn, L. Pfeiffer, and J. Federici, "Design and performance of singular electric field terahertz photoconducting antennas," Appl. Phys. Lett. **71**, 2076–2078 (1997).
18. T. Otsuji, M. Hanabe, and O. Ogawara, "Terahertz plasma wave resonance of two-dimensional electrons in InGaP/InGaAs/GaAs high-electron-mobility transistors," Appl. Phys. Lett. **85**, 2119–2121 (2004).
19. B. S. Williams, "Terahertz quantum-cascade lasers," Nature Photonics **517**, 517–525 (2007).
20. H. Minamide, T. Ikari, and H. Ito, "Frequency-agile terahertz-wave parametric oscillator in a ring-cavity configuration," Rev. Sci. Instrum. **80**, 123104 (2009).
21. K. Kawase, H. Minamide, K. Imai, J. Shikata, and H. Ito, "Injection-seeded terahertz-wave parametric generator with wide tunability," Appl. Phys. Lett. **80**(2), 195–197 (2002).
22. J. Shikata, K. Kawase, K. Karino, T. Taniuchi, and H. Ito, "Tunable terahertz-wave parametric oscillators using LiNbO3 and MgO : LiNbO3 crystals," IEEE Trans. Micrw. Theory Tech. **48**(4 PART 2), 653–661 (2000).
23. Y. Ishikawa, H. Minamide, T. Ikari, Y. Miura, T. Sawai and H. Ito, "Terahertz Spectroscopic Imaging of Liver Cancer using Ring Cavity THz- wave Parametric Oscillator," IEEE, 1236–1237 (2005).
24. Y. Zhao and D. G. Truhlar, "The M06 suite of density functionals for main group thermochemistry, thermochemical kinetics, noncovalent interactions, excited states, and transition elements: two new functionals and systematic testing of four M06-class functionals and 12 other function," Theor. Chem. Acc. **120**(1-3), 215–241 (2008).
25. M. Liu, Y. Seino, D. Chen, S. Inomata, S. j. Su, H. Sasabe, and J. Kido, "Blue thermally activated delayed fluorescence materials based on bis(phenylsulfonyl)benzene derivatives," Chem. Commun. **51**(91), 16353–16356 (2015).

1. Introduction

Organic light emitting diodes (OLEDs) have been increasingly investigated for next-generation light applications such as flat-panel displays, which are highly efficient, ultrathin and offer color tunability [1, 2]. Conventionally, the studies of fluorescence- and phosphorescence-based emitters represent the first and the second phase in OLED development, respectively. In recent research trends, thermally activated delayed fluorescence (TADF)-based emitters, which show a very high internal electroluminescence quantum efficiency of almost 100%, have ushered in a third phase in OLED development [3–7]. TADF molecules have a designed small energy gap between their lowest singlet excited state (S_1) and triplet state (T_1), which is favorable for thermal up-conversion of T_1 excitons into S_1 excitons [8]. In literature, the energy gaps of TADF materials were approximately $30-300$ meV [3–7], that were pretty close to the average energy of molecule at room temperature (27 meV). Owing to the delayed fluorescence process after the efficient reverse intersystem crossing (RISC), TADF-based emitters can achieve higher emission quantum yields. However, the efficiency of OLEDs are known to show serious roll-off due to exciton quenching [9–11], which is strongly influenced by molecular aggregation. Therefore, it is important to investigate the influence of differences in molecular aggregation for higher efficiency TADF-based OLEDs. In molecular aggregation, structural motions of molecules such as vibration and rotation (and elasticity) could influence the optical properties of each adjoining molecule. Resonant frequencies from these structural motions have been found to be in the terahertz range [12, 13]

Focusing on the terahertz background, the terahertz energy regions ($0.1-10$ THz, corresponding to $0.48-48$ meV) are in the middle of the electromagnetic spectrum between microwaves and near infrared. These relatively weak electromagnetic waves induce very low-energy motions, such as lattice vibration, molecular rotation, and intramolecular vibration. Therefore, terahertz spectroscopy is commonly applied for nondestructive identification of organic materials,

Optical Materials EXPRESS

e.g., pharmaceutical drugs [14], electro-optic polymers [15], and explosive compounds [16]. As practical terahertz wave sources, photocarrier acceleration in photoconducting antennae [17], plasma oscillations [18], terahertz quantum cascade lasers [19], and ring-cavity-based terahertz parametric oscillators (ring-TPOs) [20–22] have previously been developed in the 1 – 4 THz range. Above all, ring - TPOs are suitable for spectroscopic analysis because their frequencies can be quickly and easily tuned for terahertz radiation with coherency and monochromaticity. Actually, this ring-TPO based spectroscopy was applied for imaging living body [23]. Such recent developments in terahertz technology have enabled precise spectroscopic analysis of higher order structures.

In this paper, we demonstrated ring-TPO-based terahertz spectroscopy on organic TADF materials. As target materials, five important TADF materials, phenoxazine-triphenyltriazine (PXZ-TRZ) [4], 2,4,5,6-tetrakis(carbazol-9-yl)-1,3-dicyanobenzene (4CzIPN), 2,3,5,6-tetrakis(carbazol-9-yl)-1,4-dicyanobenzene (4CzTPN), 2,3,5,6-tetrakis(3,6-diphenylcarbazol-9-yl)-1,4-dicyanobenzene (4CzTPN-ph), and 4,5-bis(carbazol-9-yl)-1,2-dicyanobenzene (2CzPN) [3], were investigated in the frequency range of 0.60 – 1.60 THz. The terahertz spectroscopic investigations of these five TADF materials focused on the effects of the number of carbazoles, the carbazoles' coordination position, the types of carbazolyl units, and the difference between crystalline and noncrystalline materials. Then, the carbazolyl dicyanobenzene (CDCB) derivatives, especially 4CzIPN, were found to exhibit intrinsic absorption properties. Comparing the results with density functional theory (DFT)-based calculations revealed that each absorption property originated from the intramolecular motions of the electron donor and acceptor units. To the best of our knowledge, terahertz spectroscopy has never been attempted to investigate the structural properties of TADF materials, and this paper is the first report of this type of analysis.

2. Experiment

2.1. Organic TADF materials

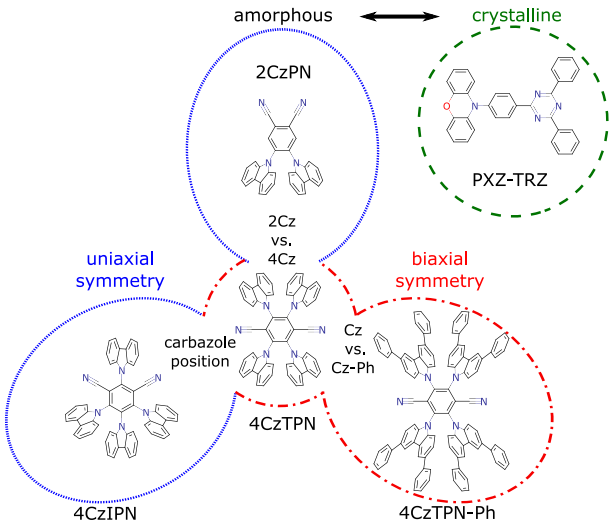

Fig. 1. Chemical structure of the five important TADF materials.

Figure 1 shows the chemical structure of the investigated TADF materials, PXZ-TRZ, 4CzTPN, 4CzTPN-Ph, 2CzPN, and 4CzIPN. The molecules enclosed in the red and blue dotted lines are the carbazolyl dicyanobenzene (CDCB) groups. The molecule groups within the red dotted line have biaxial symmetry, while the groups inside the blue line have uniaxial symme-

Optical Materials EXPRESS

try. These four materials are noncrystalline and feature carbazolyl and dicyanobenzene units. In contrast, the dotted green line indicates another type of TADF material called PXZ-TRZ. Unlike CDCBs, this material is crystalline. All of these TADF materials have very small energy gaps between the S_1 and T_1 states.

2.2. Experimental setup of ring - TPO

Figure 2 shows a schematic diagram of the experimental setup for terahertz spectroscopy. In this optical terahertz spectroscopy system, optics made of Tsurupika material (Pax Co. Ltd.) was used for the fine transmittance of terahertz waves. As a terahertz source, a ring - TPO (PHLUXi, Inc.) supporting a single frequency terahertz beam was used. The tuning range and frequency resolution of the ring - TPO were 0.60 – 1.60 THz and 0.01 THz, respectively. The terahertz beam was focused onto the sample or reference cells with a plano-convex lens (f = 25 mm, D = 30 mm Tsurupika, Pax Co. Ltd.). The transmitted beams focused onto a pyroelectric detector (PYD - 1, PHLUXi, Inc.), where the detected signals were sent to a computer through an analog-to-digital converter. The computer controlled the frequency tuning, repetition rate, and cell switching, and it synchronized at the TPO pump repetition rate of 50 Hz. The samples of TADF materials were prepared between two flat plate windows (2 mm thickness, Tsurupika, Pax. Co. Ltd.) as a pressed powder form with 100 μm thickness. The absorption coefficient was calculated by the Lambert Beer law using the frequency-domain transmittance signals of the sample and reference. All measurements were carried out at room temperature (300 K) and a humidity of 35 %. The condense of TADF powder samples were inhomogeneous owing to the condition of compression. Each sample and reference signals were measured over 400 times, furthermore, the detector signals without terahertz beam projection were measured as dark noises for 10 times. Then the average noise was extracted from each sample and reference signals. At the data processing, the error bars were calculated by the standard deviation 1σ, which means 68 % data values were included.

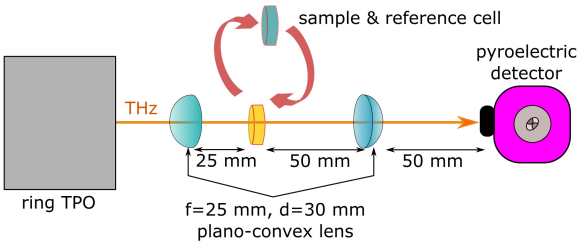

Fig. 2. A schematic diagram of terahertz spectroscopy using the TPO system.

3. Results and discussions

3.1. Absorption coefficient of TADF materials

PXZ-TRZ is one of the simply structured TADF material, which is based on a phenoxazine electron donor unit and a triphenyltriazine acceptor unit. In the literature, the donor and acceptor planes create a large dihedral angle, estimated to be 74.9°. Figure 3 shows the terahertz absorption features of PXZ-TRZ. In the measurement frequency band of 0.60 – 1.60 THz, PXZ-TRZ showed low absorption, less than 20 cm^{-1}. This result indicated that PXZ-TRZ was almost transparent in the 0.60 – 1.60 THz range.

4CzTPN - Ph has the carazole-phenyls in the carbazole position of 4CzTPN, although it has the same structural backbone as that of 4CzTPN. This material also has a biaxial molecular

Optical Materials EXPRESS

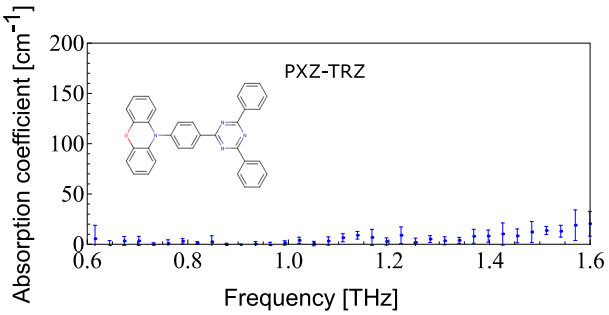

Fig. 3. The absorption coefficient of PXZ-TRZ. The experimental results are plotted with blue dots and error bars.

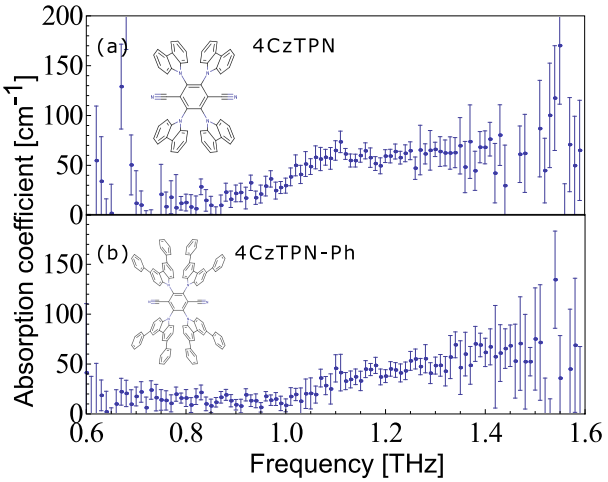

Fig. 4. The absorption coefficient of biaxial TADF materials, 4CzTPN and 4CzTPN – Ph. The experimental results are plotted with blue dots and error bars.

structure. Figure 4 shows the measured terahertz absorption characteristics of 4CzTPN and 4CzTPN - Ph. According to the results of 4CzTPN in Fig. 4(a), an absorption slope appeared over 0.9 THz due to Mie scattering because the wavelength of the terahertz beam approaches the 4CzTPN particle size. For the same reason, a scattering slope appeared over 0.9 THz for 4CzTPN - Ph, as shown in Fig. 4(b). Except for spectral fluctuations due to the S/N ratio, no other spectral features can be found in the 0.6 - 1.0 THz range for each TADF material. This result indicates that 4CzTPN and 4CzTPN - Ph have no resonant frequencies in this experiment.

2CzPN, which has a uniaxial structure, has a different number of carbazole units compared with 4CzTPN. 4CzIPN, one of the CDCB derivatives, has four carbazole electron donor units and a dicyanobenzene acceptor unit, similar to 4CzTPN. However, the donor-acceptor position is different from that of 4CzTPN. Figure 5 shows the measured terahertz absorption characteristics of 2CzPN and 4CzIPN. According to the results of 2CzPN in Fig. 5(a), 2CzPN showed high absorption characteristics. In the range of 0.60 – 1.30 THz, a large absorption slope due to Mie scattering appeared. The spectral features appeared around 1.4 – 1.5 THz, however the signal to noise ratio (S/N) is very low as seen in error bars, so that it was challenging to regard the spectrum as the characteristic absorption. On the other hand, 4CzIPN showed intrinsic absorption spectra between 0.70 – 0.90 THz, as shown in Fig. 5(b). These characteristics are different from that of Mie scattering.

Optical Materials EXPRESS

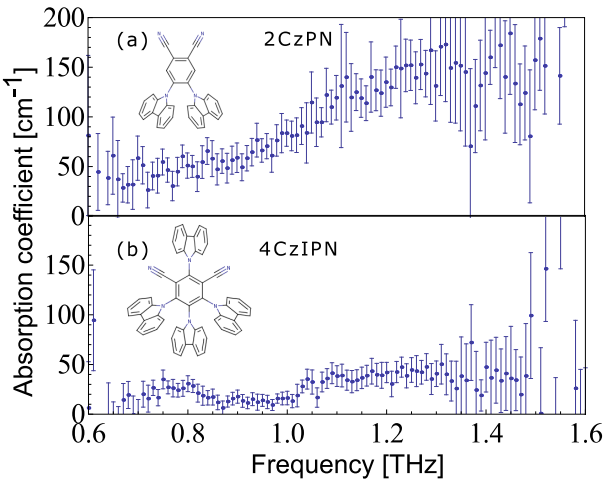

Fig. 5. The absorption coefficient of uniaxial TADF materials, 2CzPN, and 4CzIPN. The experimental results are plotted with blue dots and error bars

3.2. DFT calculations of TADF materials with CDCB derivatives

Similar results were observed in a cyclohexane solution using the same spectroscopic method (Fig. 6. This means that terahertz radiation induces not only intermolecular dynamics such as lattice vibration from the aggregation structure but also intramolecular structural motions in the TADF materials with CDCB derivatives. Therefore, it is necessary to investigate the intramolecular dynamics of a single molecule. Then, the position of the carbazole units can form intrinsic spectra for the terahertz absorption. The difference between the absorption properties of 4CzTPN and 4CzIPN is suitable to investigate the influence of the carbazole positions. For the assignments of single molecular motions, DFT calculations were carried out using Gaussian09. Calculations were performed for 4CzTPN, 4CzIPN, and 2CzPN on the ground state of single molecules using the 6-31G(d, p) basis set and the M06-2X functional [24]. The M06-2X functional, which is a hybrid meta-generalized gradient-approximation functional, reliably predicts CDCB derivatives' molecular structures [3, 25].

Figure 6 shows the DFT calculation results of uniaxial molecular materials (4CzIPN, 2CzPN) and biaxial molecular material (4CzTPN) in the 10 – 50 THz range. The vibrational-rotational resonant frequencies were plotted with the dipole strength. According to the calculation results in Fig. 6, CDCB derivatives have some of the common spectrum clouds, regardless of the rotational symmetry. Each spectrum cloud shows the dipole strength of bending the atomic bonds, which stem from the types of functional groups. In contrast, the left side of the Fig. 6 shows the low frequency resonant structures. As a result, specific differences between the resonant frequencies of 4CzIPN and 4CzTPN were confirmed. These differences can be seen in the experimental results of 4CzIPN and 4CzTPN with molecular rotational symmetry in Fig. 4(a) and Fig. 5(b). In calculation, 4CzTPN had resonant frequency around 1.0 THz, but the Mie scattering band were overlapping the spectral features. Furthermore, calculation indicated that 2CzPN had three resonant spectrum in this low frequencies, however the absorption in experiment was relatively large and S/N ratio became very low, so that it was challenging to make sure spectral features to 2CzPN. On the contrary to these two TADF materials, the resonant frequencies from the theoretical calculation agrees well with the experimental results from 4CzIPN in the range of 0.70 – 0.90 THz.

From the experimental results, 4CzIPN has specific absorption bands in the 0.7 - 0.9 THz re-

Optical Materials EXPRESS

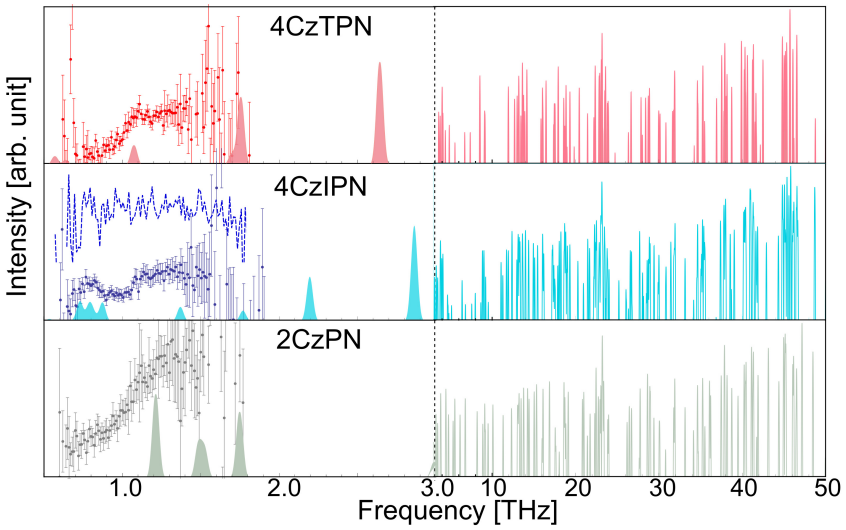

Fig. 6. DFT calculation results of biaxial and uniaxial molecules : 4CzTPN (red), 4CzTPN (blue), and 2CzPN (gray) calculated on 6-31G(d,p)/M06-2X level in low (left) and high (right) frequency ranges, compared with experimental results (dots and error bars). Absorption in cyclohexane solution (0.03 mM) were shown with blue dashed line

gion, which are differentiated by scattering. Surprisingly, the calculation results from 4CzIPN exhibited five vibrational-rotational modes at 0.695, 0.729, 0.789, 0.815, and 0.873 THz. Table 1 shows each vibrational-rotational mode and its dipole strength on 4CzIPN. Fig. 7 shows the intramolecular motion of a single 4CzIPN molecule. Comparing each experiment with the calculation results, it became clear that the 0.7 - 0.9 THz absorption bands were characterized by the motions of the carbazole units. According to Ref. [11], electron donor and acceptor units are formed with a large twist angle. These four carbazole units have rotational or butterfly motions without stretching or bending atomic bonds. Comparing each absorption spectrum of the five TADF materials and their calculation results indicates that rotational symmetries closely corresponding with the terahertz absorption of each TADF material in the 0.60 – 1.60 THz band.

Table 1. Intensities of resonant motions

Frequency [THz]	Intensity [10^{-40} esu^2 cm^2]
0.695	0.0231
0.729	0.3948
0.789	0.3213
0.815	0.1353
0.873	0.3773

Optical Materials EXPRESS

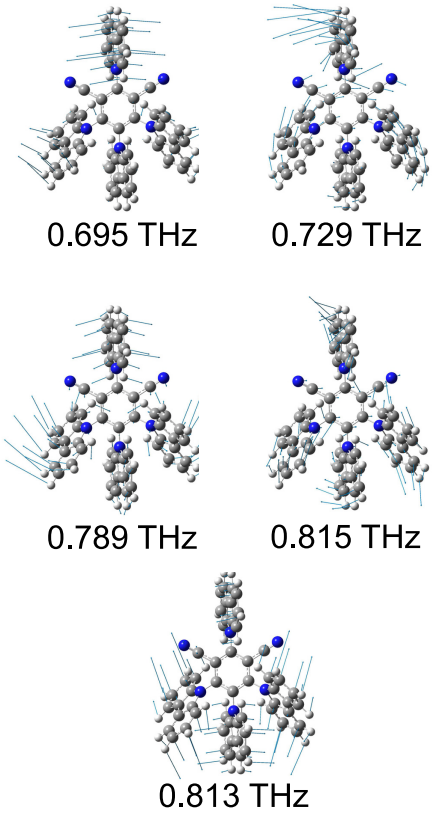

Fig. 7. Intramolecular motion of a single 4CzIPN molecule for each terahertz resonant frequency.

4. Conclusion

Using terahertz spectroscopy, five types of TADF materials, including 4CzIPN, 4CzTPN, 4CzTPN-Ph, 2CzPN, and PXZ-TRZ, were clarified to have characteristic absorption features in the 0.60 – 1.60 THz range. PXZ-TRZ, a slightly crystalline material, showed almost transparent spectral features in this spectral range. On the other hand, the CDCB group in the amorphous TADF materials showed specific absorption features corresponding to its rotational symmetries. 4CzTPN and 4CzTPN - Ph, which are biaxially symmetric molecules, indicated only scattering properties over the 1.0 THz band, while 4CzIPN, which is a uniaxially symmetric molecule, showed the specific spectral properties in the 0.7 - 0.9 THz band, in addition to the scattering. The theoretical calculations based on DFT suggested that a single 4CzIPN molecule has resonant frequencies at 0.695, 0.729, 0.789, 0.815, and 0.873 THz, which were characterized by the butterfly and rotational motions of the electron donor and acceptor units. In summary, in the 0.6 - 1.6 THz band, the amorphous TADF materials tended to show spectral features superior to those of the crystalline material. Furthermore, rotational symmetries corresponded to the intramolecular resonant motions for the CDCB group. In the future, more types of TADF material may be investigated with terahertz spectroscopy together with the study of their S_1 and T_1 states.

141.223.168.171 {ts '2019-01-31 07:58:15'}